DOI: 10.32615/ps.2019.060 PHOTOSYNTHETICA 57 (2): 458-469, 2019

Photosynthetic performance and sugar variations during key reproductive stages of soybean under potassium iodide-simulated terminal drought

D. SENGUPTA[*], S. MARRIBOINA[*], D. K. UNNIKRISHNAN[*], and A.R. REDDY[*,**,+]

Department of Plant Sciences, School of Life Sciences, University of Hyderabad, 500046 Hyderabad, India[*]
Yogi Vemana University, 516003 Kadapa, Andhra Pradesh, India[**]

Abstract

Importance of utilizing chemical desiccants to simulate terminal drought effects is gradually increasing. In the present study, a potassium iodide (KI)-simulated terminal drought stress was imposed during the full bloom (R2), pod elongation (R4), and seed initiation (R5) stages of soybean; the KI-induced desiccation effects were assessed at 1, 3, and 5 d after spraying (DASP). Plants responded to KI-simulated terminal drought stress within 1 DASP of KI-treatment, in terms of photosynthetic and transpiration rates. Seed initiation stage was found to be comparatively tolerant to KI-induced desiccation, with respect to chlorophyll degradation and PSII efficiency, which correlated well with the high hexose accumulation during this period. The present study provides a basic understanding regarding the stage-specific responses of soybean towards KI-simulated terminal drought, with respect to photosynthetic performance and sugar status and a correlation between the two traits, which could be useful for developing terminal drought-tolerant varieties.

Additional key words: chemical desiccation; *Glycine max*; hexose to sucrose ratio; linear regression; photosynthetic carbon exchange rate.

Introduction

Being the major source of edible oil, animal feed and other industrial products, soybean [*Glycine max* (L.) Merril] has become one of the most important grain legumes worldwide (Pagano and Miransari 2016). In India, soybean cultivation area increased from 0.03 Mha in 1970 to 11.67 Mha in 2016, with a corresponding increase in yield from 426 to 737 kg ha^{-1} (Agricultural Statistics at a Glance 2016). One of the major limitations to soybean productivity is the rain-fed cultivation system, with highly erratic monsoon patterns. Drastic spatio-temporal variations in rainfall often cause terminal drought stress, *i.e.*, water deprivation during the key reproductive stages, which substantially hampers the final grain yield (Daryanto *et al*. 2015). Physiologically, terminal drought effects include decreased photosynthetic carbon exchange rates (CER), early leaf senescence and maturity, and a reduced seed yield (Manavalan *et al*. 2009). Hence, the ability to remobilize stem carbohydrates towards developing pods/seeds is the key trait, which determines terminal drought tolerance in soybean. Screening and selection of cultivars with effective stem reserve mobilization marks the first step for subsequent breeding strategies for terminal drought tolerance. However, due to variation in soil moisture, field screening for terminal drought is quite difficult due to lack of uniformity and reproducibility of plant responses to the stress factor (Tuberosa 2012, Bhatia *et al*. 2014). Thus, to mimic terminal drought stress effects, chemical desiccants, such as potassium iodide (KI) were used (Regan *et al*. 1993, Royo and Blaco 1998, Bhatia *et al.* 2014). KI was reported to act as a contact desiccant and rapidly inhibits photosynthesis without showing any direct toxic effect to grain filling from the translocated carbohydrates (Nicolas and Turner 1993). The possible mechanism behind KI-induced desiccation is the interference with plant water relations. Hygroscopicity of the salt solution was also included as one of the major factors causing 'hydraulic activation of stomata' (HAS), which affects the stomatal conductance, transpiration rates, and ultimately photosynthesis (Burkhardt 2010). Also, desiccation leads to osmotic stress and triggers osmotic stress-inducible gene expression (Shapiguzov *et al*. 2005). Detailed physiochemical responses of soybean to KI-induced desiccation, with respect to specific reproductive growth stage, are not yet reported. Moreover, for wide

---

Received 28 May 2018, *accepted* 14 November 2018.

[+]Corresponding author; phone:+91 4023134508, fax: +91 4023010120, e-mail: attipalli.reddy@gmail.com

Abbreviations: CER – carbon exchange rate; Chl – chlorophyll; DASP – days after spraying; DMSO – dimethyl sulfoxide; H/S – hexose to sucrose ratio; Kn – nonphotochemical deexcitation rate constant; Kp –photochemical deexcitation rate constant; PDA – photodiode array; ΔV_{OJ} – kinetic difference of variable fluorescence between phase O and J with respect to 1 day control; ΔV_{OK} – kinetic difference of variable fluorescence between phase O and K with respect to 1 day control; $\delta_{(Ro)}$ – reduction efficiency/electron transport; $\Phi_{(Po)}$ – trapping/absorbance; $\psi_{(Eo)}$ – electron transport/trapping.

Acknowledgements: The present work is supported by the Young Scientist Start-Up grant to Dr. Debashree Sengupta (YSS/2015/000635) from Science and Engineering Research Board (SERB), a statutory body of Department of Science and Technology (DST), Govt. of India. Sureshbabu Marriboina acknowledges the fellowship from University Grant Commission (UGC), Govt. of India.

scale adoption of the technique, it is necessary to analyse and experimentally validate the plant responses to KI-simulated drought, at both physiological and biochemical levels.

As the primary plant metabolic process, photosynthesis is the 'hub', which controls all other metabolic and regulatory functions of the plant system under optimal as well as adverse environmental conditions (Lawlor and Cornic 2002, Reddy *et al*. 2004, Ashraf and Harris 2013, Flexas *et al*. 2014). During terminal drought, along with reduction in CER, leaf senescence is also triggered (Samarah *et al.* 2009, Saeidi and Abdoli 2015). It is reported that senescence itself is highly regulated and can contribute towards stress tolerance (Munné-Bosch and Alegre 2004, Jagadish *et al*. 2015). Further, sink strength variations from flowering (R1–R2) to complete seed fill (R5) also regulates the source photosynthetic capacity. Hence, KI-based terminal drought stress responses need to be analysed carefully with respect to growth stages, taking into consideration possible interactions between leaf senescence and sink strength. Apart from the actual CER, photosynthetic performance of plant is also characterized by the PSII efficiency, which is monitored *via* the chlorophyll (Chl) *a* fluorescence transients (Govindjee 2004, Boureima *et al*. 2012, Brestic *et al*. 2015). In fact, monitoring Chl *a* fluorescence has become one of the crucial nondestructive techniques for screening drought tolerance in plants, and is used extensively for screening purposes (Oukkaroum *et al*. 2007). Systematic analysis of fast kinetics of Chl *a* fluorescence provides information on quantum yield efficiency of PSII, electron transport from PSII to PSI, reduction of the end electron acceptor, photochemical and nonphotochemical quenching along with energy connectivity among PSII units, and stability of the oxygen-evolving complex (Strasser *et al*. 2004, Papageorgiou *et al*. 2007, Stirbet *et al.* 2018). For a complete understanding of the physiological responses of soybean to KI-simulated drought stress, it is necessary to evaluate the modulations in Chl *a* fluorescence patterns along with CER. Moreover, detailed stage-specific analysis of KI-desiccation effects on Chl *a* fluorescence kinetics in soybean has not been reported yet.

In general, drought stress inhibits photosynthetic rate and also disrupts carbohydrate metabolism in leaves, which together results in reduced availability of photosynthates for sink-translocation and hence, leads to seed abortion and yield loss (Nguyen *et al*. 2010, Lemoine *et al*. 2013, Osorio *et al*. 2014). As terminal drought tolerance primarily deals with reserve mobilization, either from stem or from senescing leaves, it is inevitable to analyse sugar accumulation patterns under KI-simulated drought stress. Also, it is evidenced that a sugar status plays a regulatory role in determining plant's metabolic responses under various adverse environmental conditions (Rosa *et al*. 2009, Smeekens and Hellmann 2014). Abiotic stress-induced changes in soluble sugars contents are the result of alteration in CO_2 assimilation, source-to-sink carbon partitioning, activity of sugar-metabolizing enzymes or expression of specific genes (Gupta and Kaur 2005, Baena-González *et al*. 2007). Hexose (mainly glucose and fructose) and sucrose concentrations plays crucial signalling roles for regulating metabolic processes in both source and sink tissues (Ruan 2012, Lemoine *et al*. 2013, Griffiths *et al*. 2016). Further, hexose to sucrose ratio (H/S) is also implicated as a key signalling factor regulating various aspects of plant growth and development, where high H/S ratio was reported to favour cell division and the low H/S to induce cellular differentiation (Weber *et al*. 1998, Koch 2004, Ruan *et al*. 2010, Eveland and Jackson 2012). The absolute concentration of leaf sucrose is governed by a number of concurrent factors including the rate of photosynthesis, photosynthetic carbon partitioning between starch and sucrose, sucrose hydrolysis, sucrose export rates, and drought-induced disproportions in any of the above factors will cause a change in the H/S ratio. Hence, it is important to have an insight into the pattern of hexose, sucrose, as well as H/S ratio upon KI-simulated terminal drought stress during specific reproductive stages of soybean. Previous studies have reported that under drought conditions, sucrose is accumulated due to the reduced activity of sucrose-cleaving enzyme, acid invertase. Though hexose concentrations were also reported to be enhanced under water deprivation, the amount of sucrose accumulation was comparatively higher and as a result, the H/S ratios were found to be lower under drought conditions (Zinselmeier *et al*. 1999, Andersen *et al*. 2002). KI-induced desiccation causes early senescence along with photosynthetic inhibition and it is known that during senescence reduced photosynthesis triggers metabolic reprogramming to maintain sugar homeostasis (Biswal and Pandey 2018). Hence, it is important to understand the stage-specific modulations in hexose and sucrose contents under KI-simulated terminal drought.

In the present study, we aimed to analyse the stage-specific responses of soybean to KI-simulated terminal drought stress from full bloom to seed initiation. Soybean response was analysed through modulations in the photosynthetic CER, transpiration rate, pigment composition, and various PSII efficiency parameters, along with the stage-specific sugar accumulation patterns. We also aimed to deduce a statistical correlation between the sugar status in terms of H/S ratio and the photosynthetic efficiency. Outcomes from the present study can provide a basic understanding of the usefulness of KI as a terminal drought simulator and the stage-specific variations in terminal drought response of soybean with respect to photosynthetic efficiency and sugar dynamics.

Materials and methods

Plant material and experimental conditions: The experimental material used, *Glycine max* (L.) Merril var. JS335 (Jawahar Soybean-335) is a semi-determinate and early maturing (~ 99 d) soybean variety, which is widely cultivated in India. The study was carried out in the greenhouse of University of Hyderabad, Telangana state, India (17.3°10'N and 78°23'E at an altitude of 542.6 m above mean sea level). The greenhouse conditions were as follows: PPFD ranged from 900–1,200 µmol(photon) m^{-2} s^{-1}, air temperature of 24 ± 1°C (~ 5:00–6:00 h) to

36 ± 4°C (~ 12:00–14:00 h), and relative humidity of 36 (± 5)–48 (± 2)%. Seeds were germinated in 2-L pots, filled with a mixture of red soil and manure. Commercial *Bradyrhizobium japonicum* in the powdered form (*Rhizopowder*, *AgriLife Pvt Ltd.*, India) was mixed with the seeds before sowing. Plants were maintained under regular watering regimes till flowering (*ca.* 45 d). For the present study, reproductive stages, *i.e.*, R2 (full bloom), R4 (pod elongation), and R5 (seed initiation) were selected for the 0.1% potassium iodide (KI) spray treatment, which simulates drought stress. Spray treatment (100 mL of 0.1% KI per plant) was given to three individual plants at the starting of each reproductive stage (R2, R4, and R5) and subsequent readings as well as sample collections were performed at 1, 3, and 5 DASP for each growth stage. Controls were sprayed with equal amount of double distilled water and are considered as initial or 0 DASP.

Leaf relative water content (RWC): Fresh mass (FM) of leaf samples were recorded immediately after sample collection from three different plants of control and treated groups. Leaf samples are then rehydrated in distilled water at 4°C for 24 h in order to obtain the corresponding turgid mass (TM). After recording the TM, leaves were oven-dried for 24 h to get the dry mass (DM) values. Leaf relative water content was calculated using the formula RWC [%] = [(FM) – (DM)/(TM) – (DM)] ×100.

Photosynthetic CER and transpiration rates (*E*): CER and *E* were measured using *Q-Box CO650* CO_2 exchange measurement system (*Qubit Systems Inc.*, Canada). Measurements were taken on fully expanded, mature leaves of three different plants, after applying a light intensity (white light) of 1,200 μmol(photon) m^{-2} s^{-1} for 2 min. All measurements were taken under atmospheric CO_2 conditions. Photosynthetic CO_2-fixation rate (or the carbon-exchange rate) expressed as μmol(CO_2) m^{-2} s^{-1} was calculated by the *LoggerPro* software (*Qubit Systems Inc.*, Canada) by using the differential CO_2 concentration, which is the difference between the influx and efflux CO_2 (dif. CO_2) following light exposure and the molecular flow (MF) rate. Following formulas were used for calculation:

MF = Flow rate/[22.4 × (273 + Tair)/273]/60 × 10,000/ leaf area,

CER = dif. CO_2 × MF

Transpiration rate (*E*) was also calculated automatically by the software by using the values of reference and analytical relative humidity (RH) values.

Chl *a* fluorescence transients and flux ratios: Three leaves from three different plants were dark-adapted for 30 min using leaf clips and the fluorescence intensities were recorded using a portable *Handy PEA* (*Plant Efficiency Analyzer-2126*, *Hansatech Instruments Ltd.*, Kings Lynn Norfolk, UK). Dark-adapted leaves were illuminated with a saturating light impulse of 3,000 μmol(photon) m^{-2} s^{-1}, provided by an array of three light emitting diodes, for 1 s which is sufficient to ensure closure of all PSII reaction centres. The *Handy PEA* data were analysed using the *Biolyzer* software. Three key PSII flux ratios or quantum yield parameters, *i.e.*, (*1*) TR/ABS (trapping/absorbance), which is also denoted as $\Phi_{(Po)}$ and calculated as $1 - F_0/F_m$, (*2*) ET/TR (electron transport/trapping) also denoted as $\psi_{(Eo)}$, calculated as $1 - V_j$, and (*3*) RE/ET (reduction efficiency/electron transport) or $\delta_{(Ro)}$ was calculated as $(1 - V_j)(1 - V_i)$, were selected for the present analysis which illustrates the PSII efficiency from photon capture to the reduction of the end electron acceptor in the thylakoid membrane. Further, patterns of nonphotochemical and photochemical quenching were also investigated using the deexcitation constants Kn and Kp values, respectively, which are obtained directly from the *Biolyzer* software. Analysis of Chl *a* fluorescence transients for O–K and O–J phases was performed by normalizing the variable fluorescence between O and K, as well as O and J phases of the OJIP curve [F1 (50μs) and F3 (300μs) for O–K; F1 (50μs) to F4 (2 ms) for O–J] by using the *Biolyzer* software. Theoretically, $V_{OK} = [(F_t - F_O)/(F_K - F_O)]$ and $V_{OJ} = [(F_t - F_O)/(F_J - F_O)]$, while the corresponding kinetic differences, ΔV_{OK} and ΔV_{OJ} were calculated from the normalized data by subtracting the '1 DASP control' values from the fluorescence values of each of the subsequent DASP of control and KI-treated groups, to get the L (in ΔV_{OK}) and K-bands (ΔV_{OJ}), respectively. Data presented are average of three independent replicates.

Chl pigments: Leaf samples (50 mg) were used for extraction of pigments by following dimethyl sulfoxide (DMSO) method described by Hiscox and Israelstam (1979) with minor modifications. Each leaf disc was kept in an Eppendorf tube and 2 mL of DMSO was added to each vial. Eppendorfs were kept at room temperature under dark conditions for 2 d. Then supernatant was removed through centrifugation. Absorbance of the supernatant was measured at 663.2 and 646.8 nm using *UV-Visible 160A* spectrophotometer (*Shimadzu*, Tokyo, Japan) and Chl contents were calculated using the following formula: Chl *a*: $12.25 \times A_{663.2} - 2.79 \times A_{646.8}$; Chl *b*: $21.5 \times A_{646.8} - 5.1 \times A_{663.2}$ and the results were expressed as mg g^{-1}(FM).

HPLC-based sugar estimation: Sugars (glucose, fructose, and sucrose) were extracted by following the method of Giannoccaro *et al.* (2006) with minor modifications. Briefly, 100 mg of dried and powdered sample was extracted in 1 mL (1:10, w/v) of milliQ water for 15 min in a rotospin. The extracted sample was then centrifuged at 13,000 rpm for 10 min at room temperature and 500 μL of the clear supernatant was transferred to a fresh Eppendorf tube. This sample aliquot (500 μL) was then purified by adding 1.5 mL of 95% acetonitrile and mixed for 30 min in the rotospin. Sample was then centrifuged at 13,000 rpm for 10 min at room temperature. The supernatant was collected in a fresh tube and evaporated completely by keeping in a dry bath at 95°C. Residue was redissolved in 1 mL of milliQ water and filtered through 0.22-μm filter paper (*Millipore*, *Merck*) using syringe filters. Sugars were separated isocratically through reverse phase HPLC using a NH_2 column (*Shodex-Asahipak NH2P-50-4E*) with acetonitrile:water (70:30, v/v) as a mobile phase. Flow rate was set to 1 ml min^{-1} and the absorbance was detected at 190 nm (UV) using a photodiode array (PDA) detector. Glucose, fructose, and sucrose peaks were identified through spiking with internal standards and the concentrations were calculated using external standard calibration method. Calibration curves for glucose, fructose, and sucrose were made using 0.5, 1, 2, 5, 10, 15, and 20 mg mL^{-1} concentrations and respective slope and intercepts from the straight line equations were used for calculating the concentrations from the 'area' of the HPLC peaks of the respective sugars.

Statistical analysis and linear regression modelling: All physiological measurements and biochemical estimations were performed in triplicates**.** Statistical significance between control and treated groups at each sampling time of individual reproductive stage were analysed through *Student*'s *t*-test using *SigmaPlot 11.0* and significant difference having $*p<0.05$ were considered. Linear regression models were generated using the average values of 1, 3, and 5 DASP from control and treated groups for each of the three growth stages ($n = 18$) for the response variable CER, *E*, and H/S using *SigmaPlot 11.0*.

Results

KI-simulated terminal drought impact on leaf RWC, photosynthetic CER, and transpiration rate (*E*): As KI is known to induce gradual desiccation (Sawhney and Singh 2002), we monitored the leaf RWC at 1, 3, and 5 DASP and correspondingly checked the photosynthetic CER and *E*. In the present study, leaf RWC declined gradually from 1 to 5 DASP upon KI spray, for each individual stage (R2 to R5), however, the statistically significant difference was observed from 3 DASP onwards during R2 (Fig. 1*A*) and at 5 DASP in R4 (Fig. 1*B*) and R5 stages (Fig. 1*C*). The corresponding CER values were significantly reduced to almost 50% of the control during 1 DASP of KI spray with no further progressive decline in the subsequent DASP, upon KI treatment in all three stages (Fig. 1*D–F*). A similar pattern was observed in *E*, which also declined considerably during 1 DASP and did not show any progressive decline in all the three stages (Fig. 1*G–I*).

Effect of chemical desiccation on pigment composition: Similar to natural drought conditions, KI treatment also enhanced the Chl *a*/*b* ratios consistently during 3 and 5 DASP of KI treatment at R2 and R4 stages (Fig. 2*A*,*B*), while in the R5 stage, the ratio was significantly higher than that of controls from 1 DASP onwards (Fig. 2*C*). Total Chl content declined gradually from 1 to 5 DASP of KI spray during R2, R4, and R5 stages of soybean development, however, when compared to respective controls, it was observed that at 1 DASP, total Chl content was slightly higher, but then declined during 3 and 5 DASP (Fig. 2*D–F*). To have further insight into the pigment system efficiency upon KI-induced drought stress, we analysed the PSII flux ratios or the quantum yields. The TR/ABS or $\Phi_{(Po)}$, also known as the PSII quantum yield, was found to decline at 5 DASP upon KI spray during R2 and R5 stages and at 3 and 5 DASP during R4 stage (Fig. 2*G–I*).

Effects of KI spray on quantum yield efficiencies and Chl *a* fluorescence transients: The flux ratio ET/TR (calculated as 1 – Vj) denotes the quantum yield of electron transport from PSII to PSI and is also denoted as

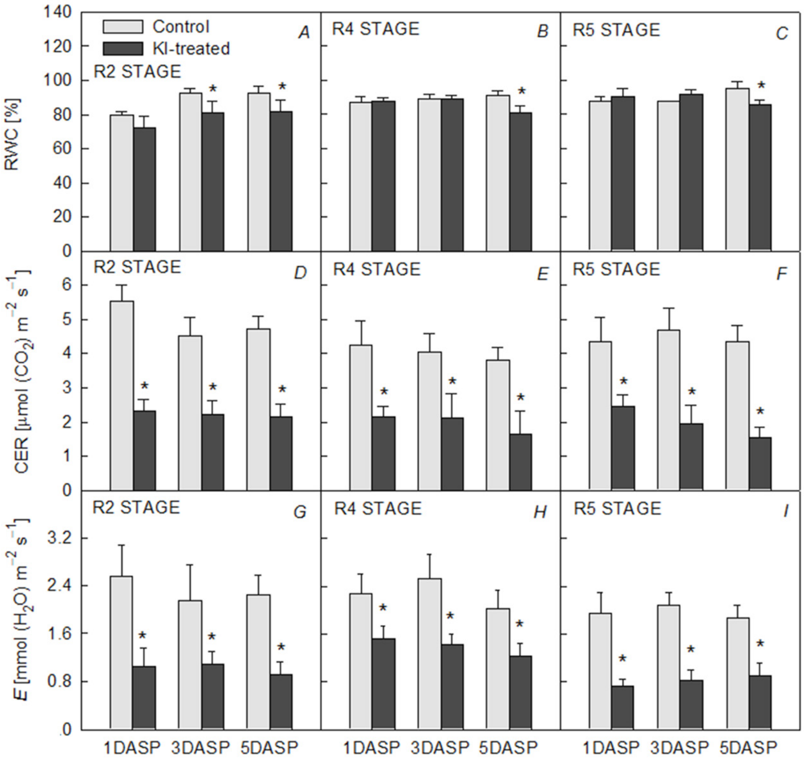

Fig. 1. Changes in the leaf relative water content (RWC) (*A–C*), photosynthetic carbon-exchange rate (CER) (*D–F*), and transpiration rate (*E*) (*G–I*) during 1, 3, and 5 d after spraying (DASP) of soybean plants with KI spray at full bloom (R2), pod elongation (R4), and seed initiation (R5) stage. Values are means ± SD ($n = 3$). * means significant difference with respect to control. $*p<0.05$.

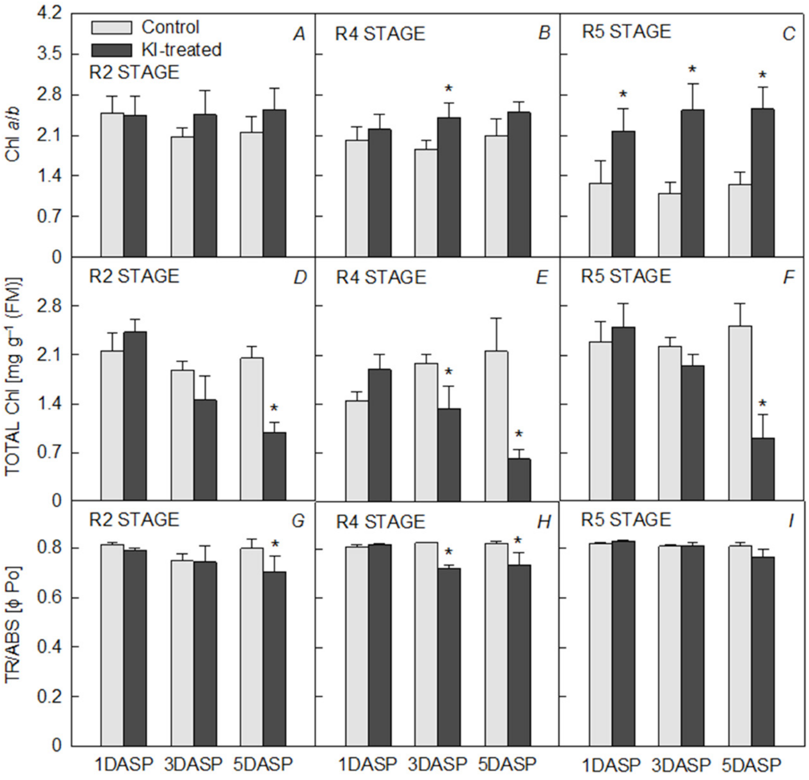

Fig. 2. Chlorophyll (Chl) *a*/*b* ratio (*A*–*C*), total chlorophyll content (*D*–*F*), and quantum yield of trapping ($\Phi_{(Po)}$) (*G*–*I*) during 1, 3, and 5 d after spraying (DASP) of soybean plants with KI spray at full bloom (R2), pod elongation (R4), and seed initiation (R5) stage. Values are means ± SD (*n* = 3). * $p<0.05$

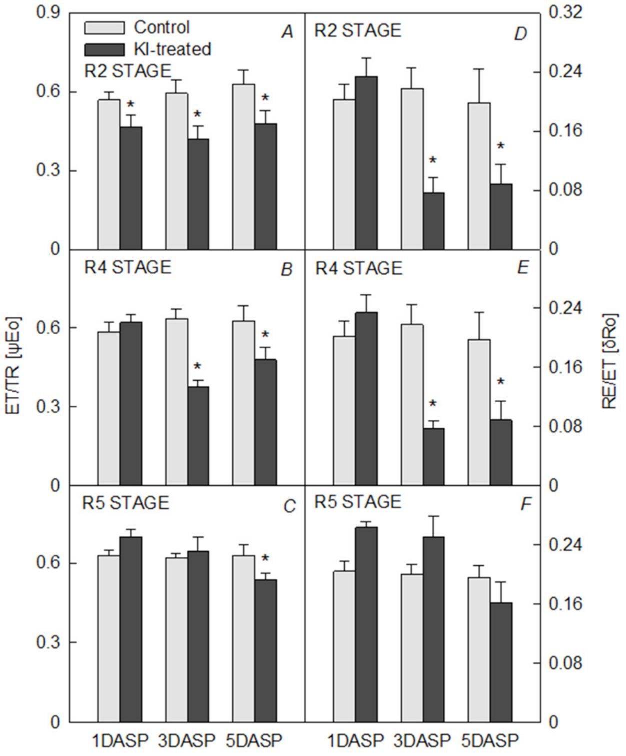

Fig. 3. Effect of KI-simulated drought stress on the quantum yield of electron transport from PSII to PSI (ET/TR, ψ_{Eo}) (*A*–*C*) and quantum yield for the reduction efficiency of the end electron acceptor (RE/ET, δ_{Ro}) (*D*–*F*) during 1, 3, and 5 d after spraying (DASP) of soybean plants with KI spray at full bloom (R2), pod elongation (R4), and seed initiation (R5) stage. Values represent mean ± SD (*n* = 3). * $p<0.05$

$\psi_{(Eo)}$. It was observed that $\psi_{(Eo)}$ declined significantly from 1 DASP onwards upon KI spray during R2 stage, after 3 and 5 DASP during R4 stage, and only at 5 DASP during R5 stage (Fig. 3*A*–*C*). The efficiency of the reduction of the end electron acceptor was indicated by the quantum yield for reduction efficiency, RE/ET or $\delta_{(Ro)}$. Here, we observed that $\delta_{(Ro)}$ decreased significantly during 3 and 5 DASP of KI treatment in both R2 and R4 stages of development (Fig. 3*D*,*E*). However, $\delta_{(Ro)}$ declined only marginally at 5 DASP of KI spray during R5 stage (Fig. 3*F*). The photochemical and nonphotochemical deexcitation rate constants (Kp and Kn) showed antagonistic response upon KI treatment. During R2 and R4 stages, Kp declined significantly from 3 DASP onwards when compared to controls. On the other hand, Kn was found to be enhanced, when compared to respective controls from 3 DASP onwards upon KI spray during R2 stage. However, during R4, Kn increased significantly during 3 and 5 DASP (Fig. 4*A*–*C*). Upon KI treatment during R5 stage, Kp showed a slight decline during 5 DASP and Kn enhanced at the same time (Fig. 4*D*–*F*).

The double normalized variable fluorescence transients between O to K phase $[(F_t - F_O)/(F_K - F_O)]$ and the corresponding kinetic difference ΔV_{OK} (Fig. 5*A*–*C*) with respect to 1 DASP control as a reference point, showed L-band during 3 and 5 DASP of KI treatment at R2 and R4 growth stages, while KI spray at R5 stage showed a significant L-band only after 5 DASP. Moreover, during

R2 stage, L-band at 5 DASP had higher amplitude than that at 3 DASP, while during R4 stage, the L-band amplitude was higher at 3 DASP. Similarly through O–J double normalization $[(F_t - F_O)/(F_J - F_O)]$ and corresponding kinetic difference, ΔV_{OJ}, positive K-bands were observed with gradually increasing amplitudes from 1 to 5 DASP of KI spray at R2 stage. During R4 stage, KI treatment showed positive K-band at 3 and 5 DASP, wherein the amplitude for 3 DASP was higher than that of 5 DASP, while at R5 stage, a positive K-band was observed only at 5 DASP of KI-induced drought stress (Fig. 5*D–F*).

KI effect on stage-specific sugar accumulation and H/S ratio patterns: Sugar accumulation was represented in terms of hexoses, which indicates the cumulative glucose (G) and fructose (F) content, sucrose contents, and the corresponding hexose to sucrose ratios (H/S) for each reproductive stage under KI-simulated terminal drought stress (Table 1). It was observed that hexose contents gradually declined with plant development from R2 to R5 stage under control conditions, however, under KI-simulated drought conditions, this trend was not followed. Further, KI-treatment resulted in higher hexose accumulation in all stages. Similar to hexoses, sucrose contents also progressively declined with reproductive development of soybean from R2 to R5 stages under non-stress conditions, but not under KI treatment. Also, enhanced sucrose accumulation was observed upon KI treatment during all stages, however, R2 stage showed significantly lesser increment in sucrose contents when compared to R4 and R5 stages. Under control conditions, the H/S ratio remained more or less stable during reproductive development from R2 to R5 stage during

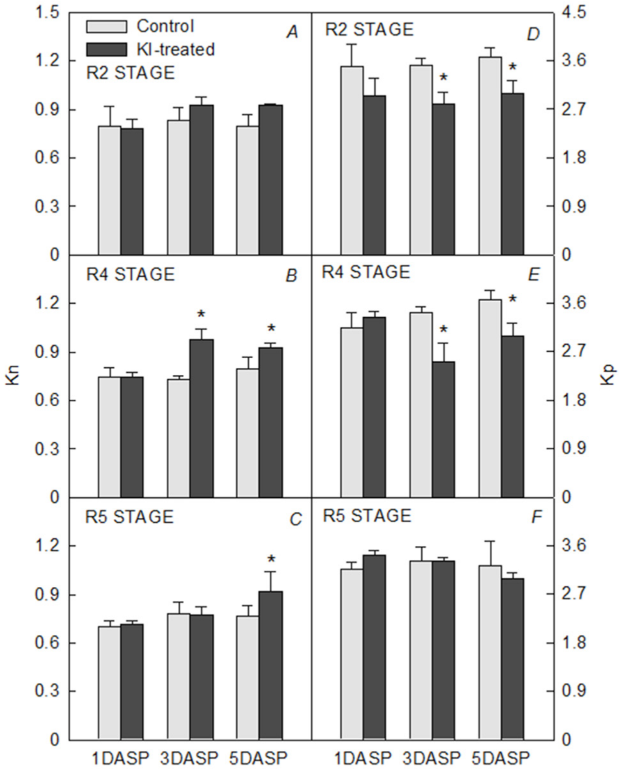

Fig. 4. The nonphotochemical (Kn) (*A–C*) and photochemical (Kp) (*D–F*) deexcitation rate constants during 1, 3, and 5 d after spraying (DASP) of soybean plants with KI spray at full bloom (R2), pod elongation (R4), and seed initiation (R5) stage. Values are mean +- S.D. *$p<0.05$

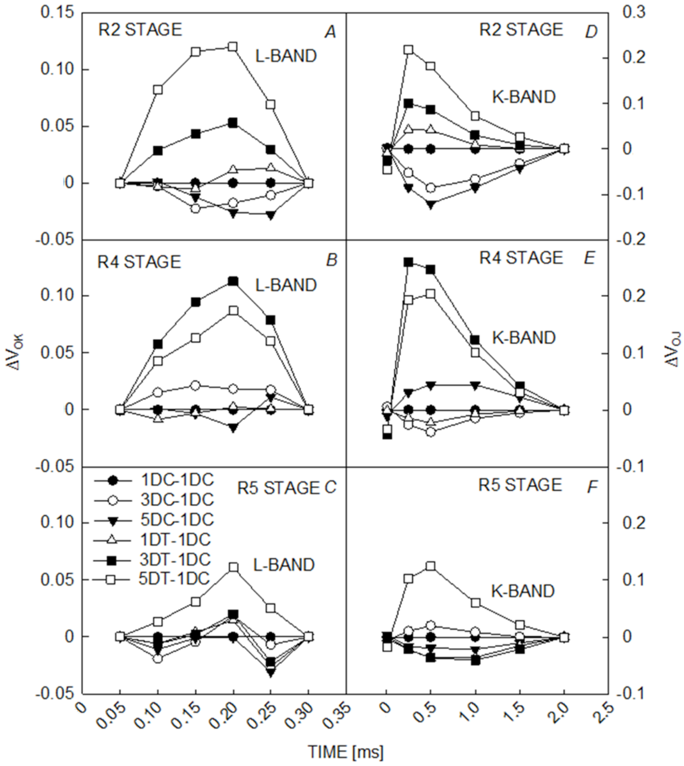

Fig. 5. Chl *a* fluorescence transients for O–K and O–J phase in soybean leaves upon KI-simulated drought stress during full bloom (R2), pod elongation (R4), and seed initiation (R5) stages. Kinetic difference of V_{OK} (ΔV_{OK}) with respect to 1 day after spraying (DASP) control (1 DC) as reference, showing prominent L-band (*A–C*). Kinetic difference of V_{OJ} (ΔV_{OJ}) with respect to 1 DASP control (1 DC) as reference, showing prominent K-band (*D–F*). Values are average of three independent replicates.

Table 1. Pattern of hexose, sucrose accumulation, and hexose to sucrose ratio (H/S) upon KI-simulated terminal drought stress at full bloom (R2), pod elongation (R4), and seed initiation (R5) stages of soybean development. Values are means ± SD (n = 3).* indicates significance at $p<0.05$, ns – not significant, DASP – days after spraying. ^{a}H/S ratio is represented as the mean(hexose)/mean(sucrose) and hence SD and statistical significance are not included.

Parameter	Growth stage	1 DASP		3 DASP		5 DASP	
		Control	KI-treated	Control	KI-treated	Control	KI-treated
Hexose [mg g^{-1}(DM)]	R2	71.6 ± 6.7	99.1 ± 7.5*	78.4 ± 3.6	96.2 ± 5.8*	75.7 ± 8.1	91.5 ± 4.9*
	R4	43.5 ± 3.7	45.3 ± 5.1^{ns}	41.7 ± 2.2	55.7 ± 3.6*	47.7 ± 3.4	66.8 ± 4.8*
	R5	32.9 ± 2.8	106.5 ± 10.4*	35.0 ± 5.4	106.1 ± 5.7*	30.6 ± 7.3	98.2 ± 3.2*
Sucrose [mg g^{-1}(DM)]	R2	9.5 ± 1.1	9.7 ± 0.9^{ns}	9.9 ± 0.6	12.1 ± 0.8*	9.1 ± 1.1	14.0 ± 1.7*
	R4	5.0 ± 1.6	34.4 ± 2.3*	5.2 ± 1.5	35.1 ± 3.7*	6.1 ± 2.1	70.4 ± 8.2*
	R5	3.4 ± 2.9	41.8 ± 5.8*	4.2 ± 3.1	44.0 ± 1.9*	3.8 ± 3.9	31.5 ± 7.4*
H/S ratio^{a}	R2	7.5	10.1	7.9	7.9	8.2	6.5
	R4	8.6	1.3	8.0	1.6	7.8	0.9
	R5	9.7	2.5	8.2	2.4	7.9	3.1

all observation points. Upon KI-induced desiccation, H/S ratio declined significantly in R4 and R5 stages during all DASP observed, when compared to respective controls. However, at R2 stage, the ratio was higher in comparison to controls at 1 DASP, similar at 3 DASP, and slightly lower at 5 DASP.

Overall stage-specific sugar accumulation, pigment efficiency, and carbon assimilation patterns: Since sugar accumulation pattern did not follow any specific pattern with progressing DASP of KI spray treatment, we analysed the overall (an average of the 3 observations points, *i.e.*, 1, 3, and 5 DASP) pattern of sugar accumulation and H/S ratio for each individual stage of reproductive development. To get a comprehensive overview, along with sugar accumulation, we also analysed the pigment efficiency in terms of the overall stage-specific total Chl content, functional reaction centres (RC/CS$_o$) and the quantum yield of energy trapping (TR/ABS) as well as the carbon-assimilation efficiency defined with respect to quantum yield of electron transport from PSII to PSI (ET/TR), reduction efficiency for the final electron acceptor (RE/ET), and the actual carbon exchange rates (CER) in response to KI-induced drought stress. In the present study, we observed that hexose (G+F) concentrations showed a more or less gradual decline with stage progression from R2 to R5 under control conditions. Upon KI treatment, hexose contents were enhanced in all stages (Fig. 6*A*). Sucrose contents also declined gradually from R2 to R5 stage under control conditions. But, with KI-induced drought stress, sucrose accumulation increased and was found to be significantly higher than that of controls at R4 and R5 stages of development (Fig. 6*B*). On the other hand, hexose to sucrose ratios (H/S) were significantly lower than that of controls during R4 and R5 stage, remained similar to controls at R2 stage (Fig. 6*D*). Overall, the total Chl content declined upon KI treatment during R2 and R4 but remained similar to controls during R5 stage (Fig. 6*E*). Similarly, the overall RC/CS$_o$ declined with KI treatment during R2 and R4 but remained stable during R5 stage (Fig. 6*C*). On average, the yield determining the light capturing efficiency, TR/ABS, remained stable in response to KI-induced drought in all growth stages except R2, which showed a slight decline (Fig. 6*G*). Both ET/TR and RE/ET declined significantly with KI treatment during R2 and R4 stages but remained unchanged during R5 stage (Fig. 6*H*,*I*). The photosynthetic CER showed an overall decrease upon KI treatment during all the growth stages when compared to controls (Fig. 6*F*).

Linear regression model for correlating H/S ratio with photosynthetic efficiency: In order to deduce a possible inter-relationship between the photosynthetic CER, stomatal conductance, and leaf H/S ratio, we considered the average values for each of the three observation points (1, 3, and 5 DASP) under control and KI-treated plants, at a particular reproductive growth stage (R2, R4, and R5) as dataset (n = 18) and carried out three linear regression modelling: (*1*) between CER and E, (*2*) CER and H/S, and (*3*) E and H/S using *SigmaPlot 11.0*. The regression analysis depicted that CER *vs.* E had the highest R^2 value (0.808), followed by CER *vs.* H/S (0.473), while E *vs.* H/S showed the minimum R^2 value (0.302). All the statistical details including correlation coefficients for the regression analyses are provided in Table S1 (*supplement*). The linear regression analyses are depicted graphically in Fig. 7*A*–*C*.

Discussion

Dependency on seasonal rains for cultivation of major crops, including soybean, often imposes the risk of encountering terminal drought stress, which results in huge decline in crop productivity (Sadras 2002, Samarah *et al.* 2009). Developing terminal drought tolerant varieties through breeding or genetic engineering approach requires extensive screening for terminal drought tolerance traits among cultivars/wild relatives and a proper understanding of the underlying physiological, biochemical, and molecular mechanisms. At the onset of grain filling, chemical desiccation of plant canopies

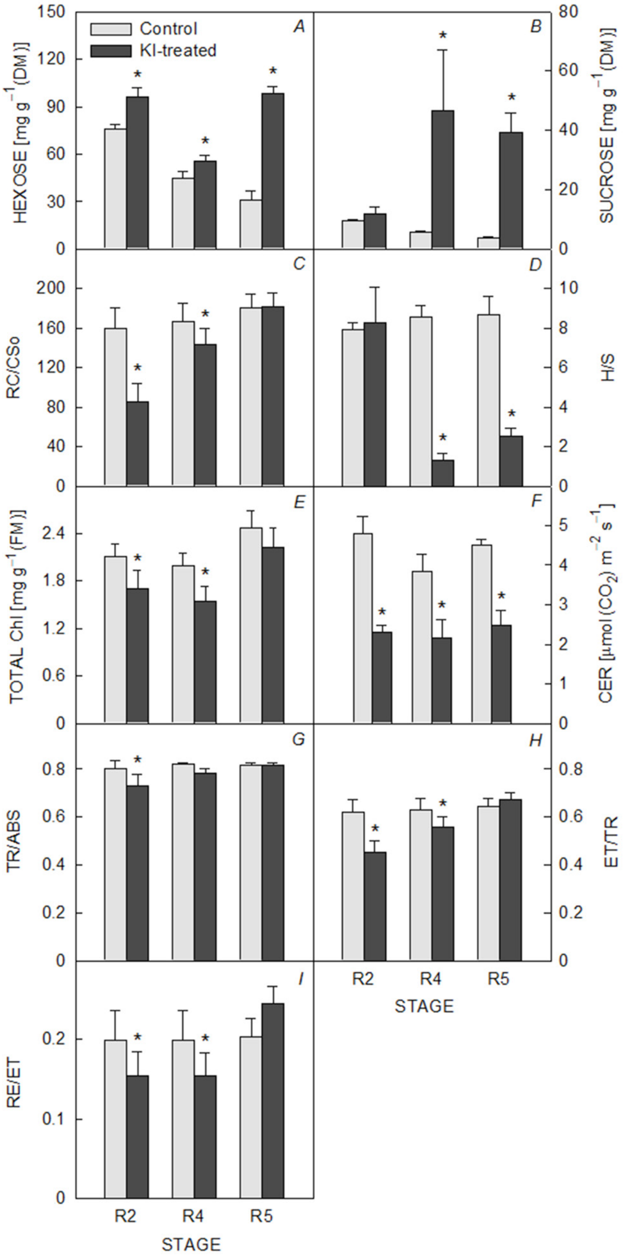

Fig. 6. Stage-specific accumulation patterns of hexose (*A*), sucrose (*B*), number of functional reaction centres per cross section area (RC/CS_o) (*C*), hexose to sucrose ratio (H/S) (*D*), total chlorophyll content (*E*), carbon-exchange rate (CER) (*F*), quantum yield efficiency of PSII (TR/ABS) (*G*), quantum yield of electron transport from PSII to PSI (ET/TR) (*H*), and reduction efficiency of the final electron acceptor (RE/ET) (*I*) in soybean plants with KI spray at full bloom (R2), pod elongation (R4), and seed initiation (R5) stage. Values represent mean ± SD (*n* = 3). *$p<0.05$

was long suggested as a tool for analysing genotypic differences in stem reserve-mediated grain filling, when current photosynthesis is limited (Blum *et al.* 1983) and KI was reported to act as a contact desiccant (Tyagi *et al.* 2000). Previous studies reported that KI-induced desiccation leads to a decreased Chl content, stomatal conductance, transpiration, photosynthetic rates, and induces early senescence and maturity (Royo and Blanco 1998, Sawhney and Singh 2002, Bhatia *et al.* 2014), which closely simulates terminal drought stress symptoms and hence, is proposed as a potential tool for screening terminal drought tolerance in field crops (Nezhad *et al.* 2012, Ongom *et al.* 2016). Also, drying initiates several major alterations in the carbohydrate metabolism, which might directly or indirectly correlate with desiccation tolerance. Present study involved a detailed stage-specific analysis of KI-simulated terminal drought responses in soybean with respect to photosynthetic physiology and sugar status.

Soybean is known to be most susceptible to water-deficit conditions during germination and reproductive stages (Liu *et al.* 2004, Angra *et al.* 2010). Occurrence of drought during full bloom and pod initiation (R2 and R4) stages of soybean induces flower/pod abortion causing significant decline in seed number and the effect is irreversible upon return of normal water conditions (Ruan *et al.* 2010), whereas water limitation during seed-filling stage (R5) results in seed abortion or low seed mass due to reduced photosynthate transfer to these structures (Borrás *et al.* 2004). Usefulness of KI, as a simulator of drought stress during reproductive stages, is established in rice, wheat, and recently in soybean as well (Singh *et al.* 2012, Kordenaeej *et al.* 2013, Bhatia *et al.* 2014). However, most of the studies characterizing the use of KI-simulated terminal drought stress concentrated on KI impact at a final yield stage or 6 to 7 d after spray with a few reports examining the plant responses within 1 DASP (Sawhney and Singh 2002). No reports have come up till date on detailed physiological and biochemical characterization of KI-simulated terminal drought responses in soybean.

In the present study, we observed that photosynthetic CER and *E* declined significantly within 1 DASP of KI-spray treatment, even though the total Chl content quantum yield (TR/ABS), Chl *a*/*b* ratio, and RC/CS_o remained unaffected (statistically insignificant) at 1 DASP for all the growth stages. As hygroscopicity of chemical desiccants, such as KI, was postulated to interfere with plant water relations and also the fact that cuticular and stomatal pathway for salt entry into plants is possible (Burkhardt 2010), we can hypothesize that physical deposition of KI on leaf surface interfered with stomatal conductance. This could be the reason behind the significant decline in CER and *E* after 1 DASP, when the corresponding RWC did not decline significantly. This hypothesis is also supported by the correlation coefficient analysis from the regression between CER and *E*, CER and H/S, and *E* and H/S, where the correlation coefficient as well as significance was maximal for regression between CER and *E*, followed by CER and H/S, while the correlation coefficient between *E* and H/S was the lowest. This supports the hypothesis that KI deposition on leaf surface caused closing of stomata leading to decrease in CER. At the same time, hexose and sucrose contents were also enhanced within 1 DASP of KI-spray during R2, R4 as well as R5 stages. Accumulation of hexoses under drought stress is a well-known plant osmotic regulation to withstand the decreasing water potential in the tissues (Hare *et al.* 1998,

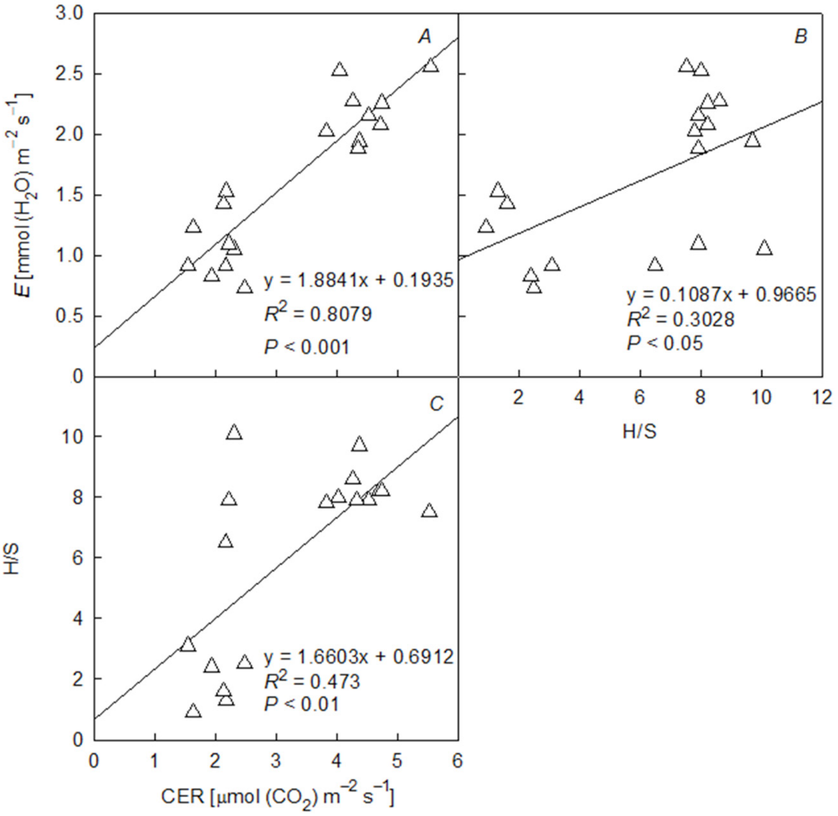

Fig. 7. Scatter plot for the linear regression analysis between carbon-exchange rate (CER) and transpiration rate (*E*) (*A*), hexose to sucrose ratio (H/S) and *E* (*B*), and CER and H/S (*C*).

Liu *et al.* 2004, Wang *et al.* 2016), which could be the result of higher invertase activity (Andersen *et al.* 2002, Fu *et al.* 2010) or enhanced starch degradation (Pelleschi *et al.* 1997, Lemoine *et al.* 2013). Previous studies on impact of drought stress on carbohydrate composition in soybean showed a significant decline in leaf sucrose content (Liu *et al.* 2004). However, in the present study, upon KI-induced desiccation, a significant increase in the sucrose content was observed. Higher sucrose accumulation with KI-simulated drought stress was also reported in wheat (Sawhney and Singh 2002), which can be attributed to a number of factors including higher partitioning of photosynthates towards sucrose rather than starch, impaired translocation of assimilated sucrose to sink tissues or utilizing the osmoregulatory functions of sucrose under desiccation stress. Also, irritation-induced electrical signals were reported to inactivate H^+-sucrose symporters, which reduces sucrose transport from leaves to phloem cells (Sukhov 2016). We can hypothesize that a similar mechanism operates under KI-induced desiccation resulting in a higher sucrose accumulation. In fact, the lowered photosynthetic CER within 1 DASP of KI spray, observed in the present study, could be due to the high hexose and sucrose accumulation in leaves, which is known to suppress photosynthesis through Rubisco inhibition (Goldschmidt and Huber 1992).

When compared to hexose contents, sucrose accumulation was found to be higher under KI-simulated drought stress during R4 and R5 stages, resulting in low H/S ratio when compared to controls. However, R2 stage showed a relatively lesser increase in sucrose leading to a higher H/S ratio at 1 DASP, similar at 3 DASP, and slightly lower ratio at 5 DASP with respect to controls. Comparatively lower sucrose accumulation at R2 stage can be attributed to rapid sucrose translocation to newly developed flowers at full-bloom stage, which upon gradual abortion showed progressive decline in the H/S ratio. It has been reported that the water demand in soybean during the flowering stage is the highest (Liu *et al.* 2003, Rosolem 2005) and leaf carbohydrate status is implicated in regulating the process of flower or pod abortion under natural drought conditions (Liu *et al.* 2004). It has been shown that H/S ratio plays a key role in regulating reproductive development of plants (Weber *et al.* 1998). A higher H/S ratio favors cell division during early stages of reproductive development, while a lower H/S ratio (or high sucrose content) is suggested to induce maturity and differentiation during later stages (Wang and Ruan 2013). Drought stress is reported to cause a decline in H/S ratio in pod and flowers of soybean, which was assumed to be one of the factors for pod/flower abortion due to reduced cell division (Liu *et al.* 2004). Importance of H/S ratio in leaf apoplasm has been described for mediating hormone-regulated leaf senescence, wherein a decreased H/S ratio due to lower cell wall invertase (CWIN) activity in the leaf apoplasm was hypothesized to trigger abscisic acid-mediated leaf senescence along with induction of cysteine protease genes (Ruan *et al.* 2010). As KI-simulated terminal drought stress is known to induce early senescence symptoms in plants, our results support the above hypothesis. In order to analyse whether H/S ratio correlates with photosynthetic CER during reproductive development of soybean, we made a simple regression analysis using H/S ratio as the independent and CER as the dependent variable. A highly significant positive correlation was observed between the two parameters. Though the R^2 for the regression was only 0.473, it was highly significant as the P value was 0.002, *i.e.*, $P<0.01$. Sugar signals, especially hexose and sucrose, and/or H/S ratio-based are constantly found to be involved in modulating various photosynthesis-related parameters (Goldschmidt and Huber 1992, Iglesias *et al*. 2002, Lemoine *et al*. 2013). The actual concentrations of independent total hexose (glucose + fructose) and sucrose also correlated significantly with CER, just as H/S ratio. However, as the main objective of the present study was to show the role of H/S ratio, only the H/S and CER regression analysis is shown here. Hence, the present statistical correlation and modelling of H/S-based regulation of CER indicates that H/S ratio along with actual concentrations of hexose and sucrose plays a role in modulating photosynthetic performance of plants under terminal drought. Further validation of the model will require large-scale experimental inputs in this regard.

A strong inter-relationship exists between sink demand and source supply, which regulates the overall photosynthetic performance of plants during various growth stages (Paul and Foyer 2001). For a careful investigation of the KI-simulated terminal drought stress on stage-specific photosynthetic responses, Chl *a* fluorescence transients and quantum yield (flux ratios) were monitored simultaneously with CER and sugar status dynamics. The KI-induced senescence effects were evidenced in the present study by the observed gradual decrease in total Chl content. Lower energy connectivity among PSII units (higher L-band) and disrupted oxygen-evolving complex (higher K-band) were previously implicated as severe drought stress effects (Sengupta *et al*. 2013, Kalaji *et al*. 2016, Falqueto *et al*. 2017) and in the present study positive L and K-bands were observed during 3 and 5 DASP of KI spray at R2 and R4 stages, while only at 5 DASP (with comparatively lower amplitude) during R5 stage. Also, the quantum yield for electron transport from PSII to PSI, efficiency of reduction of the end electron acceptor and PSII quantum yield were significantly affected during KI-simulated terminal drought stress at R2 and R4 stages, but not R5 stage. Similar results were reported in wheat leaves in response to salt stress (Mehta *et al.* 2010). Our data demonstrates that KI-induced desiccation created a progressive damage to PSII stability during all the three stages, however, R5 stage exhibited relative tolerance. The observed maintenance in PSII efficiencies in R5 stage during 1 and 3 DASP of KI treatments correlated with the comparatively higher hexose accumulation during this period, which might act as osmoticum for tolerating the KI-induced desiccation damage at R5.

In conclusion, the present study demonstrated that soybean responded to KI-simulated terminal drought stress within 24 h of treatment, however, the desiccation impact was progressive in nature. Also, the H/S ratio could act as a key predictor of photosynthetic CER during reproductive stages of soybean under terminal drought stress. Further, seed initiation stage (R5) was found to be comparatively tolerant to KI-induced terminal drought stress with respect to Chl degradation and PSII efficiency, which correlated well with high hexose accumulation during this period. Outcomes from the present study not only elaborated the usefulness of utilizing KI spray as an agent for simulating terminal drought stress in soybean but also provided information on stage-specific response of soybean to terminal drought stress and highlighted the importance of the H/S ratio in predicting photosynthetic efficiency during terminal drought stress. However, future research is required to establish the molecular mechanisms underlying such physiological responses to KI-simulated terminal drought stress.

References

Agricultural Statistics at a Glance 2016. Available at eands.dacnet.nic.in/PDF/Glance-2016.pdf, 2016.

Andersen M.N., Asch F., Wu Y. *et al.*: Soluble invertase expression is an early target of drought stress during the critical, abortion-sensitive phase of young ovary development in maize. – Plant Physiol. **130**: 591-604, 2002.

Angra S., Kaur S., Singh K. *et al.*: Water-deficit stress during seed filling in contrasting soybean genotypes: Association of stress sensitivity with profiles of osmolytes and antioxidants. – Int. J. Agr. Res. **5**: 328-345, 2010.

Ashraf M., Harris P.J.C.: Photosynthesis under stressful environments: An overview. – Photosynthetica **51**: 163-190, 2013.

Baena-González E., Rolland F., Thevelein J.M. *et al.*: A central integrator of transcription networks in plant stress and energy signalling. – Nature **448**: 938-942, 2007.

Bhatia V.S., Jumrani K., Pandey J.P.: Evaluation of the usefulness of senescing agent potassium iodide (KI) as a screening tool for tolerance to terminal drought in soybean. – Plant Know. J. **3**: 23-30, 2014.

Biswal B., Pandey J.K.: Loss of photosynthesis signals a metabolic reprogramming to sustain sugar homeostasis during senescence of green leaves: Role of cell wall hydrolases. – Photosynthetica **56**: 404-410, 2018.

Blum A., Poyarkova H., Golan G., Mayer J.: Chemical desiccation of wheat plants as a simulator of post-anthesis stress. I. Effects on translocation and kernel growth. – Field Crop. Res. **6**: 51-58, 1983.

Borrás L., Slafer G.A., Otegui M.A.: Seed dry mass response to source-sink manipulations in wheat, maize and soybean: a quantitative reappraisal. – Field Crop. Res. **86**: 131-146, 2004.

Boureima S., Oukkaroum A., Diouf M. *et al.*: Screening for drought tolerance in mutant germplasm of sesame (*Sesamum indicum*) probing by chlorophyll *a* fluorescence. – Environ. Exp. Bot. **81**: 37-43, 2012.

Brestic M., Zivcak M., Kunderlikova K. *et al.*: Low PSI content limits the photoprotection of PSI and PSII in early growth stages of chlorophyll *b*-deficient wheat mutant lines. – Photosynth. Res. **125**: 151-166, 2015.

Burkhardt J.: Hygroscopic particles on leaves: nutrients or desiccants? – Ecol. Monogr. **80**: 369-399, 2010.

Daryanto S., Wang L., Jacinthe P.-A.: Global synthesis of drought effects on food legume production. – PLoS ONE **10**: doi: 10.1371/journal.pone.0127401, 2015.

Eveland A.L., Jackson D.P.: Sugars, signalling and plant development. – J. Exp. Bot. **63**: 3367-3377, 2012.

Falqueto A.R., da Silva Júnior R.A., Gomes M.T.G. *et al.*: Effects of drought stress on chlorophyll *a* fluorescence in two rubber tree clones. – Sci. Hortic.-Amsterdam **224**: 238-243, 2017.

Flexas J.A., Diaz-Espejo A., Gago J. *et al.*: Photosynthetic limitations in Mediterranean plants: A review. – Environ. Exp. Bot. **103**: 12-23, 2014.

Fu J., Huang B., Fry J.: Osmotic potential, sucrose level, and activity of sucrose metabolic enzymes in tall fescue in response to deficit irrigation. – J. Am. Soc. Hortic. Sci. **135**: 506-510, 2010.

Giannoccaro E., Wang Y.-J., Chen P.: Effects of solvent, temperature, time, solvent to sample ratio, sample size, and defatting on the extraction of soluble sugars in soybean. – J. Food Sci. **71**: 59-64, 2006.

Goldschmidt E.E., Huber S.C.: Regulation of photosynthesis by end-product accumulation in leaves of plants storing starch, sucrose, and hexose sugars. – Plant Physiol. **99**: 1443-1448, 1992.

Govindjee: Chlorophyll *a* fluorescence: A bit of basics and history. – In: Papageorgiou G.C., Govindjee (ed.): Chlorophyll *a* Fluorescence: A Signature of Photosynthesis. Pp. 1-42. Kluwer Academic, Dordrecht 2004.

Griffiths C.A., Paul M.J., Foyer C.H.: Metabolite transport and associated sugar signalling systems underpinning source/sink interactions. – Biochim. Biophys. Acta **1857**: 1715-1725, 2016.

Gupta A.K., Kaur N.: Sugar signalling and gene expression in relation to carbohydrate metabolism under abiotic stresses in plants. – J. Biosciences **30**: 761-776, 2005.

Hare P.D., Cress W.A., Van Staden J.A.: Dissecting the roles of osmolyte accumulation during stress. – Plant Cell Environ. **21**: 535-553, 1998.

Hiscox J.D., Israelstam G.F.: A method for the extraction of chlorophyll from leaf tissue without maceration. – Can. J. Botany **57**: 1332-1334, 1979.

Iglesias D.J., Lliso I., Tadeo F.R., Talon M.: Regulation of photosynthesis through source: sink imbalance in citrus is mediated by carbohydrate content in leaves. – Physiol. Plantarum **116**: 563-572, 2002.

Jagadish K.S.V., Kishor P.B.K., Bahuguna R.N. *et al.*: Staying alive or going to die during terminal senescence: An enigma surrounding yield stability. – Front. Plant Sci. **6**: doi: 10.3389/fpls.2015.01070, 2015.

Kalaji H.M., Jajoo A., Oukarroum A. *et al.*: Chlorophyll *a* fluorescence as a tool to monitor physiological status of plants under abiotic stress conditions. – Acta Physiol. Plant. **38**: doi: 10.1007/s11738-016-2113-y, 2016.

Koch K.: Sucrose metabolism: regulatory mechanisms and pivotal roles in sugar sensing and plant development. – Curr. Opin. Plant Biol. **7**: 235-246, 2004.

Kordenaeej A., Nejad A.A.N., Shojaeian A.A. *et al.*: Simulating the effect of terminal drought stress by potassium iodide and its use in mapping QTLs for yield and yield components in bread wheat. – Int. J. Agr. Plant Prod. **4**: 659-663, 2013.

Lawlor D.W., Cornic G.: Photosynthetic carbon assimilation and associated metabolism in relation to water deficits in higher plants. – Plant Cell Environ. **2**: 275-294, 2002.

Lemoine R., La Camera S., Atanassova R. *et al.*: Source to sink transport of sugar and regulation by environmental factors. – Front. Plant Sci. **4**: doi: 10.3389/fpls.2013.00272, 2013.

Liu F., Andersen M.N., Jensen C.R.: Loss of pod set caused by drought stress is associated with water status and ABA content of reproductive structures in soybean. – Funct. Plant Biol. **30**: 271-280, 2003.

Liu F., Jensen C.R., Andersen M.N.: Drought stress effect on carbohydrate concentration in soybean leaves and pods during early reproductive development: its implication in altering pod set. – Field Crop. Res. **86**: 1-13, 2004.

Manavalan L.P., Guttikonda S.K., Tran L.S.P. *et al.*: Physiological and molecular approaches to improve drought resistance in soybean. – Plant Cell Physiol. **50**: 1260-1276, 2009.

Mehta P., Allakhverdiev S.I., Jajoo A.: Characterization of photosystem II heterogeneity in response to high salt stress in wheat leaves (*Triticum aestivum*). – Photosynth. Res. **105**: 249-255, 2010.

Munné-Bosch S., Alegre L.: Die and let live: leaf senescence contributes to plant survival under drought stress. – Funct. Plant Biol. **31**: 203-216, 2004.

Nezhad K.Z., Weber W.E., Röder M.S. *et al.*: QTL analysis for thousand-grain weight under terminal drought stress in bread wheat (*Triticum aestivum* L.). – Euphytica **186**: 127-138, 2012.

Nguyen G.N., Hailstones D.L., Wilkes M. *et al*: Drought stress: Role of carbohydrate metabolism in drought-induced male sterility in rice anthers. – J. Agron. Crop Sci. **196**: 346-357, 2010.

Nicolas M.E., Turner N.C.: Use of chemical desiccants and senescing agents to select wheat lines maintaining stable grain size during post-anthesis drought. – Field Crop. Res. **31**: 155-171, 1993.

Ongom P.O., Volenec J.J., Ejeta G.: Selection for drought tolerance in sorghum using desiccants to simulate post-anthesis drought stress. – Field Crop. Res. **198**: 312-321, 2016.

Osorio S., Ruan Y.L., Fernie A.R.: An update on source-to-sink carbon partitioning in tomato. – Front. Plant Sci. **5**: doi: 10.3389/fpls.2014.00516, 2014.

Oukkaroum, A., Madidi, S.E., Schansker, G., Strasser, R.J.: Probing the responses of barley cultivars (*Hordeum vulgare* L.) by chlorophyll *a* fluorescence OLKJIP under drought stress and re-watering. – Environ. Exp. Bot. **60**: 438-446, 2007.

Pagano, M.C., Miransari, M.: The importance of soybean production worldwide. – In: Miransari, M. (ed.): Abiotic and Biotic Stresses in Soybean Production. Pp. 1-26. Academic Press, Amsterdam 2016.

Papageorgiou G.C., Tsimilli-Michael M., Stamatakis S.: The fast and slow kinetics of chlorophyll *a* fluorescence induction in plants, algae and cyanobacteria: a viewpoint. – Photosynth. Res. **94**: 275-290, 2007.

Paul M.J., Foyer C.H.: Sink regulation of photosynthesis. – J. Exp. Bot. **52**: 1383-1400, 2001.

Pelleschi S., Rocher J.P., Prioul, J.L.: Effect of water restriction on carbohydrate metabolism and photosynthesis in mature maize leaves. – Plant Cell Environ. **20**: 493-503, 1997.

Reddy A.R., Chaitanya K.V., Vivekanandan M.: Drought-induced responses of photosynthesis and antioxidant metabolism in higher plants. – J. Plant Physiol. **161**: 1189-1202, 2004.

Regan K.L., Whan B.R., Turner N.C.: Evaluation of chemical desiccant as a selection technique for drought resistance in a dry land wheat breeding programme. – Aust. J. Agr. Res. **44**: 1683-1691, 1993.

Rosa M., Prado C., Podazza G. *et al.*: Soluble sugars – metabolism, sensing and abiotic stress, a complex network in the life of plants. – Plant Signal. Behav. **4**: 388-393, 2009.

Rosolem C.A.: {Role of Brazil in fighting hunger in the World.] – In: Suzuki S., Yuyama, M.M., Camacho, S.A.: [Bulletin of Soybean Research.] Pp. 95-102. Fundação MT, Mato Grosso, Brazil 2005. [In Portuguese]

Royo C., Blanco R.: Use of potassium iodide to mimic drought stress in triticale. – Field Crop. Res. **59**: 201-212, 1998.

Ruan Y.L., Jin Y., Yang Y.J. *et al.*: Sugar input, metabolism, and signalling mediated by invertase: Roles in development, yield potential, and response to drought and heat. – Mol. Plant **3**: 942-955, 2010.

Ruan Y.L.: Signalling role of sucrose metabolism in development.

– Mol. Plant **5**: 763-765, 2012.

Sadras V.: Interaction between rainfall and nitrogen fertilisation of wheat in environments prone to terminal drought: economic and environmental risk analysis. – Field Crop. Res. **77**: 201-215, 2002.

Saeidi M., Abdoli M.: Effect of drought stress during grain filling on yield and its components, gas exchange variables, and some physiological traits of wheat cultivars. – J. Agr. Sci. Tech.-Iran **17**: 885-898, 2015.

Samarah N.H., Alqudah A.M., Amayreh J.A. *et al*.: The effect of late-terminal drought stress on yield components of four barley cultivars. – J. Agron. Crop Sci. **195**: 427-441, 2009.

Sawhney V., Singh D.P.: Effect of chemical desiccation at the post-anthesis stage on some physiological and biochemical changes in the flag leaf of contrasting wheat genotypes. – Field Crop. Res. **77**: 1-6, 2002.

Sengupta D., Guha A., Reddy A.R.: Interdependence of plant water status with photosynthetic performance and root defense responses in *Vigna radiata* (L.) Wilczek under progressive drought stress and recovery. – J. Photochem. Photobiol. **127**: 170-181, 2013.

Shapiguzov A., Lyukevich A.A., Allakhverdiev S.I. *et al*.: Osmotic shrinkage of cells of *Synechocystis* sp. PCC 6803 by water efflux *via* aquaporins regulates osmostress-inducible gene expression. – Microbiology **151**: 447-455, 2005.

Singh A.K., Singh A., Singh A.K. *et al*.: Application of potassium iodide as a new agent for screening of drought tolerance upland rice genotypes at flowering stage. – Plant Know. J. **1**: 25-32, 2012.

Smeekens S., Hellmann H.J.: Sugar sensing and signalling in plants. – Front. Plant Sci. **5**: doi: 10.3389/fpls.2014.00113, 2014.

Stirbet A., Lazár D., Kromdijk J., Govindjee: Chlorophyll *a* fluorescence induction: Can just a one-second measurement be used to quantify abiotic stress responses? – Photosynthetica **56**: 86-104, 2018.

Strasser R.J., Tsimilli-Michael M., Srivastava A.: Analysis of the chlorophyll *a* fluorescence transient. – In: Papageorgiou, G.C., Govindjee (ed.): Chlorophyll *a* Fluorescence. Advances in Photosynthesis and Respiration, Vol. 19. Pp. 321-362. Springer, Dordrecht 2004.

Sukhov V.: Electrical signals as mechanism of photosynthesis regulation in plants. – Photosynth. Res. **130**: 373-387, 2016.

Tuberosa R.: Phenotyping for drought tolerance of crops in the genomics era. – Front. Physiol. **3**: doi: 10.3389/fphys.2012.00347, 2012.

Tyagi P.K., Singh D.P., Pannu R.K.: Effect of post-anthesis desiccation on plant-water relation, canopy temperature, photosynthesis and grain yield in wheat genotypes. – Ann. Biol. **16**: 111-119, 2000.

Wang L., Ruan Y.L.: Regulation of cell division and expansion by sugar and auxin signalling. – Front. Plant Sci. **4**: doi: 10.3389/fpls.2013.00163, 2013.

Wang R., Gao M., Ji S. *et al*.: Carbon allocation, osmotic adjustment, antioxidant capacity and growth in cotton under long-term soil drought during flowering and boll-forming period. – Plant Physiol. Bioch. **107**: 137-146, 2016.

Weber H., Heim U., Golombek S. *et al*: Expression of a yeast-derived invertase in developing cotyledons of *Vicia narbonensis* alters the carbohydrate state and affects storage functions. – Plant J. **16**: 163-172, 1998.

Zinselmeier C., Jeong B.R., Boyer J.S.: Starch and the control of kernel number in maize at low water potentials. – Plant Physiol. **121**: 25-35, 1999.